

Extraction of Dynamic HDL-A Models of Thermally Based Microsystems from Physical Simulations

S. Marco, M. Carmona, J. Samitier

Departament d'Electrònica, associated unit to the CNM-CSIC, Universitat de Barcelona,
Av. Diagonal 645-647, 08028-Barcelona, Spain. santi@el.ub.es

ABSTRACT

While analyzing the behaviour of complex systems it is not practical to carry out the simulation of the complete model at the physical level. In order to move from simulations at the physical level towards system modeling with more abstract representations, it is sometimes necessary to use lumped representations of a initially continuous system. Some of these lumped elements will be represented by a black-box model defined by a certain transfer function. This work addresses the problem of the identification of a continuous system, namely a thermo-pneumatic microactuator, from its transient behavior as obtained from finite element modeling. The influence of the integration algorithms is studied and a solution is proposed to avoid its influence in the extracted transfer function. The final representation of the system is used in the simulation of a micropump by using an electronic simulator.

I. INTRODUCTION

Finite Element Analysis (FEM) is the current tool for micromechanical component designers within the microsystems discipline. However, in the simulation and design of microsystems is not practical to carry out the analysis of the complete system at the physical level. It is necessary to extract behavioral models which can describe with enough accuracy the behavior of the system currently being analyzed (1). These models will be implemented in a mixed-signal simulator which permits analog model description of electromechanical systems. While waiting for the definitive appearance of the VHDL-A standard by the 1076.1 Technical committee of the IEEE, Eldo and Saber are the most commonly simulation environments used today. While minimizing computing time and retaining the significant behavioral features such approach permits a fair important simulation point: the interaction between the electromechanical parts and the associated interface and control electronics.

In many cases it is not enough a static description of the system, and it is necessary to extract its dynamics from the FEM-simulation. When modeling subcomponents of the system with a black box approach it is first necessary to define the appropriate input and output signals. Then, for linear systems the dynamic behavior will be represented by a suitable transfer function. However, many microsystems can include considerable sources of non-linear behavior arising from geometrical non-linearity's when large deflections are present (mechanical systems), or for instance temperature

dependent material properties in thermal problems. When the system behaves in a non-linear manner it is well-known that the most accurate linear representation depends on the operating point, or more strictly, on the probability density function of the input signal. In those cases, it can be necessary to extract the transfer function from the analysis of signals in the time-domain. For such purpose the techniques of system identification can be applied to the simulated transients. However, this approach has to be exercised with care if accurate results have to be obtained while minimizing the necessary computing time. The main problems arise from: (i) the description of the system can need frequency specification over several frequency decades leading to very long transients and in-consequence very long computing times; (ii) the frequency behavior extracted from the analysis of the transients not depends just on the system behavior but on the particular integration algorithm of the differential equation.

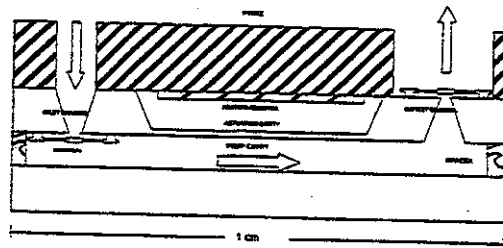


Fig. 1 Cross-sectional scheme of the micropump

These difficulties will be addressed and illustrated in the following work that is focussed on the behavioral modeling of a micromachined fluidic pump described in section II. Special care deserves the dynamical behavior of the actuation unit that is the object of the analysis. Section III introduces the Finite Element model and particular analysis that were carried out. The joint description of the analysis results and problems then encountered are the object of section IV. How the extracted model fits in the complete micropump simulation is included in section V. The conclusions of the work are going to be summarized in section VI.

II. MICROPUMP WORKING PRINCIPLE

In order to discuss the model of the micropump, we start by presenting its operation first. As it can be observed in figure 1, the micropump is thermo-pneumatically actuated by means of a integrated heater contained in the air cavity. Pulsed

power supply to this heater alternatively increases and decreases the temperature in the cavity and consequently the internal pressure. The cyclic variation of the pressure in the cavity deflects the membrane and causes the pumping action. Aided by two non-return valves, an unidirectional flow is achieved. The expected operating frequency is about 1 Hz. The micropump analyzed in this work consist in a stacking of three silicon chips and one Pyrex substrate. The objective is to deliver water flows in the range of 1-100 $\mu\text{l}/\text{min}$. On the later, a Ta_2N heating resistor is deposited. The microvalves are made of polysilicon and they consist on a valve lid supported by four arms.

III. FINITE ELEMENT ANALYSES

The aim of the analysis is to find the dynamical behavior of the actuation unit. As we have previously noted, the first point is to define the significant input and output quantities. We have selected as input magnitude the power delivered by the heating resistor. As output we selected the pressure in the actuation cavity. In this way, the output of this model fits perfectly in the total behavioral model where pressure is the across variable while volume flow is the complementary quantity. We did not selected voltage as input signal in order to maximize the number of non-linearity's included in the high level simulation. This will result in a weakly non-linear FEM analysis the results of which would be represented fairly well by a linear model.

It is clear from the stated problem that we are in front of a coupled thermo-mechanical problem where a diversity of materials play: Pyrex, silicon and air. FEM simulations were carried out using ANSYS. This commercial code supports the transient analysis where the individual time-steps can be fully non-linear thermo-mechanical analysis. Furthermore, this code permits the simulation of the contained air in the actuation cavity. The sources of non-linearity are mainly the temperature dependence of properties as thermal conductivity, heat capacity and expansion coefficients.

In order to carry out, the subsequent identification procedure the input signal selected was a random binary signal (RBS) with values 0W or 1.2W. These are the expected values for the input signal in the normal operation of the actuation unit.

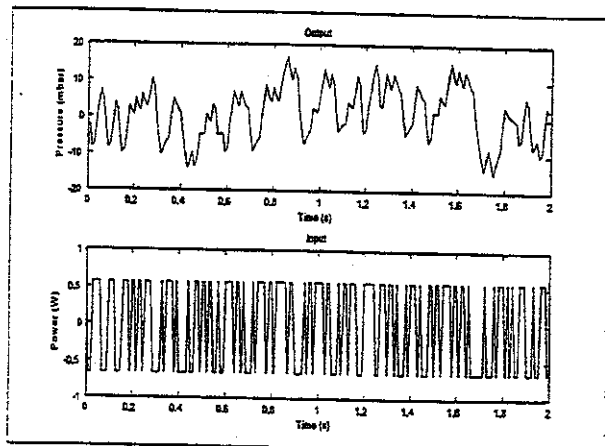


Fig. 2 Input and output signals of the simulated system. Step time 0.01s. Mean values have been subtracted.

A previous analysis was carried out to extract the response to a 1 Hz square wave. From its inspection an approximate time constant of 0.5 s was observed. For this reason we selected 2s as the total transient time with a time step of 0.01s. This resulted in a 200 points transient. In order to minimize, the effect of the transient in the identification step, first the actuation unit was driven to a initial condition corresponding to an average dissipation of 0.6W, by means of a static simulation. From this point, 200 points corresponding to the RBS input were analyzed. The appearance of the input and output signals can be observed in figure 2.

IV. RESULTS AND DISCUSSION

From the FEM-simulation we had a file of data that was two hundred samples long. The first attempt for the identification of the transfer function was carried out with ARX-models (2), AutoRegressive with eXogenous input. The file was collected with sampling (simulation time-step) period 0.01s.

$$A(q)y(t) = B(q)u(t-nk) + e(t) \quad (1)$$

where $A(q)$, $B(q)$ are polinomials in the delay operator q^{-1} . The parameters are obtained by minimizing the loss function:

$$V_{LS} = \sum e(t)^2 = \sum |A(q)y(t) - B(q)u(t-nk)|^2 \quad (2)$$

Input and output data were divided into one part for estimation and a second part for validation. For estimation were chosen 150 points and the remaining 50 were used for validation. We looked for a transfer function where the error term represented less than 1% of the total output power. In addition the selected model should fulfill the conditions of whiteness of the residuals, and lack of correlation to the input signal. The best model turned out to be a transfer function with 2 poles and 2 zeros. However, we did not succeed with simple ARX models to achieve the previous requirements.

The obtained results indicated that the error term could be non-white. To take into account this possibility we chose a more complex model as follows:

$$A(q)y(t) = B(q)u(t-nk) + \frac{1}{D(q)}e(t) \quad (3)$$

Also here we were forced to look at the power of the error, the autocorrelation of the residuals and the crosscorrelation of the residuals and the input. The residuals represented less than 0.1% of the output power and they were white and uncorrelated with the input signal. The optimum model had four poles and three zeros in the transfer function of the signal and two extra poles in the transfer function of the error.

If we now take a look at the bode plot of the signal, figure 3, we see that we have a zero at the highest frequency. This has no physical meaning at all and we began to suspect that this

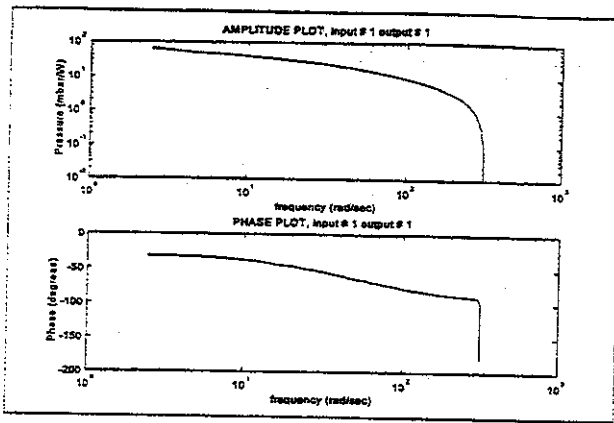


Fig. 3 Bode plot showing a zero at the highest frequency

had to do with the solution algorithm implemented in the FEM solver.

In order to examine this phenomena is interesting to take a look at the integration algorithms used in the FEM solver. Let us focus our analysis in the thermal pass of every time step. The equation to be solved should be discretized not only spatially, but also in time. The difference equation to be solved in the FEM-simulations looks as follows (3).

$$[C]\{u'_n\} + [K]\{u_n\} = \{F^n\} \quad (4)$$

where $[C]$ =Damping matrix, $[K]$ =Coefficient matrix, $\{u\}$ =vector of DOF values, $\{u'\}$ =time rate of DOF values and $\{F^n\}$ =applied load vector.

From the time point of view this can be considered as a difference equation which can be analyzed more thoroughly with the z-transform. For the integration of this difference equation the solver uses the Crank-Nickolson rule which has the following appearance:

$$\{u_{n+1}\} = \{u_n\} + (1-\theta)\Delta t\{u'_n\} + \theta\Delta t\{u'_{n+1}\} \quad (5)$$

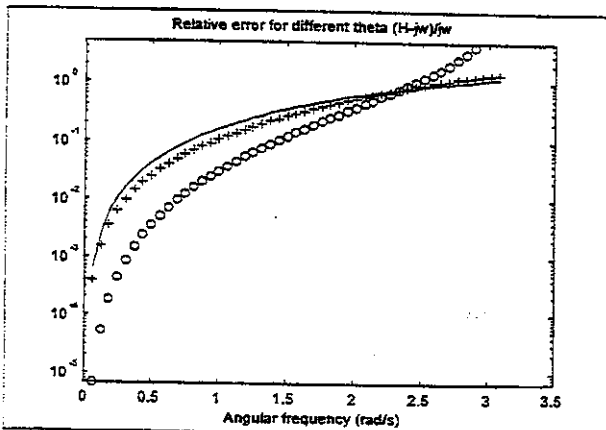


Fig. 4 Derivative error (relative to ideal) for different choices of θ : o $\theta=0.5$, + $\theta=0.75$, solid $\theta=1$.

where θ is the transient integration parameter and $\Delta t = t_{n+1} - t_n$ (timestep or sampling period) where a default value of $\theta=0.5$ is recommended. When looking at this equation one realize that the solution may depend n the transient integration parameter θ .

Substituting $\{u_{n+1}\}$ from eq 2 into eq 1 yields:

$$\left\{ \frac{1}{\theta\Delta t} [C] + [K] \right\} \{u_{n+1}\} = \left\{ F^n + [C] \left(\frac{1}{\theta\Delta t} \{u_n\} + \frac{1-\theta}{\theta} \{u'_n\} \right) \right\} \quad (6)$$

The Crank-Nickolson rule is the implicit way to approximate the time-derivative present in the heat partial differential equation. In signal processing it is well known the difficulty in trying to design a digital differentiator that accurately represent the ideal continuous behavior $H(\omega)=j\omega$. The Crank-Nicholson rule is not an exception. There exists no value of θ that accurately represents the above behavior. In the finite element theory the influence of θ has been usually analyzed by examine the step-response of the system (4). Much more information can be drawn if we analyze this in the whole frequency span of interest. In order to analyze this, let us look at the z-transform of equation 5.

$$H(z) = \frac{1-z^{-1}}{\theta + (1-\theta)z^{-1}} \quad (7)$$

For low frequencies the approximation made for solving the difference equation, numerically, holds with a relatively small error but as the frequency increases the error becomes unacceptably big. This is independent of whatever value of θ is chosen. θ is bounded by the limits $0.5 < \theta < 1.0$. In figure 4 is also shown the relative error for the different values of θ . We can clearly see in figure 4 that for low frequencies $\theta=0.5$ is the best choice. However for frequencies higher than $1/(4\Delta t)$, there is an error larger than 10%. When transforming equation 4 to the z-domain we obtain:

$$\frac{u(z)}{F(z)} = \frac{\theta[(1-\theta)z^{-1} + \theta]}{[(C+K\theta) - Cz^{-1}][1-\theta]z^{-1} + \theta} C(1-\theta)z^{-1}(1-z^{-1}) \quad (8)$$

From the visual inspection of this result it is clear that the effect of θ cannot be easily removed. But at least we observe that there is an artificial zero which depends only on the value of θ and it is not dependent of the physical problem being solved. If we take a look at the numerator of the last equation we see that we exact can determine the zeros for the different choices of θ . ($\theta < 0.5$ implies poles outside the unit circle resulting in an unstable behavior of the solution)

$$z = \frac{\theta-1}{\theta} \quad (9)$$

This yields for $\theta = 0.5$ a zero at $z = -1$ witch is exactly what we found when searching for a model in the previous section. Note that from a physical point of view, the presence of a

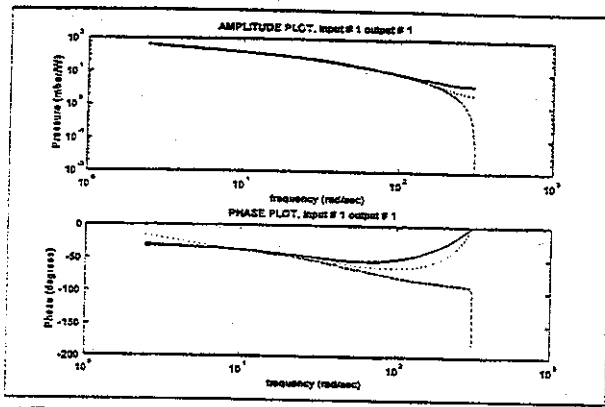


Fig. 5 Bode plot for different integration parameters.

zero exactly at the highest frequency is not plausible. Then it is clear that the solution algorithm is distorting the behavior of the system. At this point we also determined to carry out two more FEM-simulations with different values of θ . This was done in purpose to see if we would reach a different result with a different value of θ (0.75 and 1.00). As can be seen in figure 5, the three curves in the bode plot agrees quite well for low frequencies but differs a lot at higher. Here the next question that rises is: how can we obtain the final transfer function over a wide frequency span with minimum influence of the θ parameter? To answer this question we followed two procedures:

Procedure 1

Because it is clear that the approximations are better at low frequencies than at high frequencies, we decided to analyze in more detail high frequencies. An additional simulation was carried out with a sampling period of 0.001 s. and total length 0.2 s. In addition, by looking at the phase plot, figure 5, we observed that we needed to analyze also lower frequencies. An additional simulation of 20 s with a time step of 0.1 s was done. In this way we explored four decades of frequencies with just 600 simulation points. Compare with the 20000 points if the whole frequency span is to be analyzed in one single simulation span. This point has a practical importance taking into account the CPU usage of FEM simulation when realistic models are built (about 20 min. per time-step in a Sparc 10). On the other hand, this frequency splitting is going to give us an additional criteria for the goodness of the individual discrete models by looking at the connection between the different transfer functions.

It seems at this point reasonable to try to find points where it is possible to connect the different transfer functions (from different sampling periods) to obtain a non-parametric description of the complete one. By looking at figure 6 we see that in the amplitude plot we have an almost perfect overlap and we are quite free to choose connection points but the number is more limited in the phase plot. Even though it is more limited it is still possible. The points has to be chosen carefully because the next step would be to try to fit a continuous transfer function spanning from 10^{-1} to 10^3 rad/s. To get a reasonable good fit there can not exist any "jumps" in the connection points of the individual transfer function. In order to fit this continuous transfer function a non linear least

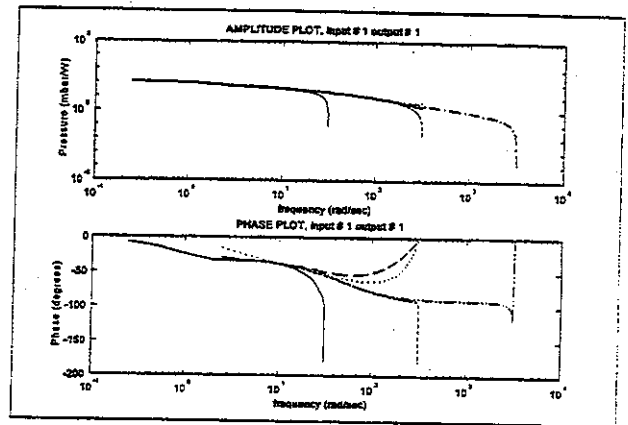


Fig. 6 Bode plot of transfer function for the five different simulations.

square fit was carried out in the frequency domain (5).

$$\Theta = \operatorname{argmin} \sum_i |H_i - H(\omega, \Theta)|^2 \quad (10)$$

where Θ is the vector of the parameters. When fitting this curve it was also necessary to weight the data so that the region with poles and zeros got the highest importance. The connected curve and the fitted curve can be seen in figure 7.

This, as can be seen, resulted in a good fit and from this fit we also obtained a expression of the transfer function. The transfer functions chosen for this connection were those obtained with $\theta=0.5$ and it seems that in this experiment this was the optimal choice. The theoretical expression for this fit has two zeros and three poles. This means that we have three time-constants. The time-constants and their respective amplitudes can be found in the table I.

Table I: Results of transfer function fitting in frequency domain or by METS analysis.

Method	Time constants(s)	Amplitudes ($^{\circ}\text{C/W}$)
Fitting in frequency domain	0.021	14.2
	0.068	23.4
	0.714	71.4
METS (10 order)	0.023	17.6
	0.062	21.5
	0.740	69.9

At this point it is curious to note that further increases in the order of the model even decreasing the mean square fitting error result in terms with negative amplitudes which have non-physical meaning. These artifacts originate probably by the concatenation of the different sections simulated with different time-steps.

This shows that by fitting together the curves with different sampling periods we have obtained the transfer function for a relatively wide frequency span.

Procedure 2)

In the second procedure we have used a uniform time step in the logarithm of time. That is, simulations are carried out at times given by:

$$t_n = t_0 \cdot 10^{\frac{n}{N}} \quad (11)$$

where N is the number of points per decade. In this way short time steps are used for fast phenomena and bigger time-steps for slow phenomena. We did the simulations with $N=20$, although posterior analysis showed that this value can be reduced up to $N=10$, without decreasing the accuracy of the analysis. The obtained curves can be analyzed by a method proposed by the authors called METS-Multi-Exponential Transient Spectroscopy. A similar procedure has been already proposed by Szekely et al.(6) This technique is based on the multi-differentiation of the transient and produces a set of peaks whose position indicates the time constant and the height of the peak indicates the amplitude of the exponential term(7).

$$METS_n(y) = \sum_{i=1}^M A_i n^i e^{-n} \exp(n(y-z_i)) - \exp(y-z_i) \quad (12)$$

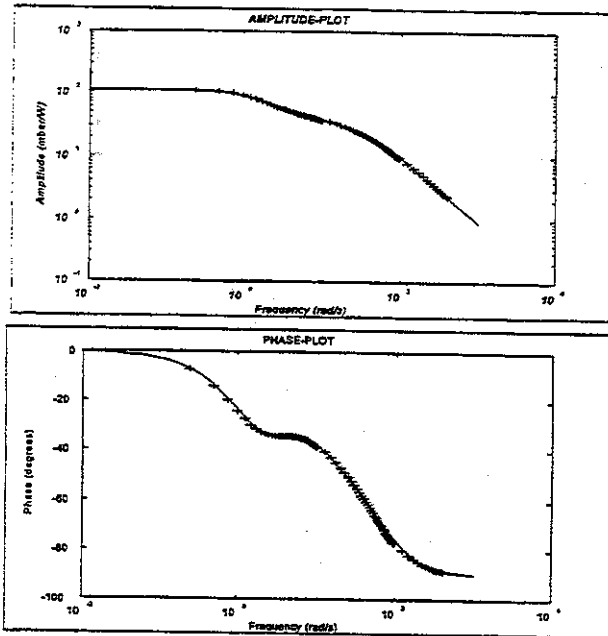


Fig. 7 Bode plot of connected and fitted transfer function

where $y = \ln(t)$ and $z_i = \ln(\tau_i)$ and A_i are the corresponding amplitudes. In figure 9, the METS signals for the simulated transient can be observed with only three time constants in agreement with the previous procedure. Table I lists the estimated amplitudes and time constants. This method is inherently more accurate because there is no need to concatenate the results of different simulations. In addition by the same automatic adjustment of the time-step the results are almost independent of the integration parameter θ . For more

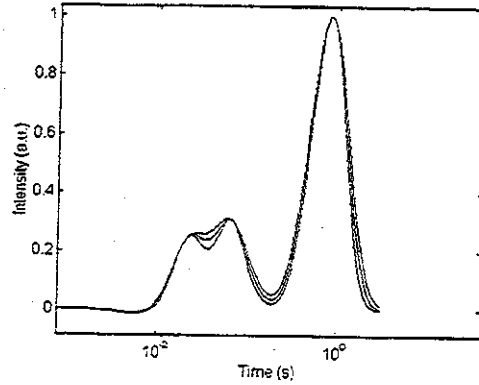


Fig. 9 10th order METS signals for the different values of the integration parameter.

information about the possibilities of the METS analysis the reader is addressed to ref. 7,8. Note that with this method we need only 40 simulation points to explore 4 time decades, compared to 600 points in procedure 1.

The analog hardware description language used for the present work (HDLA-Eldo, Mentor Graphics) permits the introduction of functional blocks described by linear transfer functions by directly writing the differential equation. This interesting possibility eliminates the necessity to extract equivalent Foster/Cauer RC networks to emulate the thermal behaviour. The HDLA model extracted from the present analysis can be observed in Table II.

V. COMPLETE BEHAVIORAL MODEL AND SIMULATION

Because the final purpose of the pump is to deliver liquid flows, the behavioral model of the micropump is based in a fluidic network with lumped models of the different components. A scheme of such a behavioral model can be seen in figure 10. Details of the extraction of lumped elements from fluidic components can be found elsewhere (7).

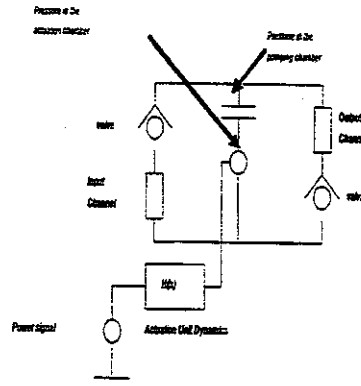


Fig. 10 Behavioral model of the micropump.

Table II: HDLA model of the actuation unit.

```

ENTITY difeq IS
  generic(tamb : real);
  PIN (pwr : nkn; defl : fluid; tp : thermal);
END;
ARCHITECTURE a OF difeq IS
  CONSTANT k,x2,x1,x0,y2,y1,y0: real;
  STATE fl,x,y,yd,ydd,xd,tt : analog;
BEGIN
  RELATION
    PROCEDURAL FOR init =>
      x2 := 50.0*949.8; x1 := 50.0*53.0e3;
      x0 := 50.0*3.0e5; y2 := 69.6; y1 := 1570.0;
      y0 := 2998.0; y := 0.0; yd := 0.0; ydd := 0.0;
      xd := 0.0; k := 0.021730;
    PROCEDURAL FOR dc,transient =>
      x := pwr.a;
      defl.fr %:= fl;
      tp.t %:= y*k + tamb;
    EQUATION (fl,ydd,yd,y,xd) FOR dc,transient =>
      y = defl.p; xd = ddt(x); yd = ddt(y);
      ydd = ddt(yd);
      ddt(ydd) + y2*ydd + y1*yd + y0*y =
      x2*ddt(xd)+x1*xd+x0*x;
    END RELATION;
  END;

```

The modeling of every subcomponent of the micropump permits to ensemble them in a complete model which has been implemented using the analog behavioral capabilities of ELDO (Anacad-Mentor Graphics Inc). The different subcomponent models have been obtained for different values of the geometrical parameters. Then it is possible to study the effect of, e.g. the hole size or the valve stiffness, in the final behavior of the pump. Figure 11 shows the transient behavior of the micropump for a mean supply power of 1 W and a frequency of 1 Hz.

VI. CONCLUSIONS

Lumped model representations of more complex systems may require the extraction of black-box models of components from simulations at the physical level. When extracting dynamic behaviors from FEM transients it is essential to be aware of the possible distortion introduced by the solver. Our work has shown how this effects appear when trying to extract the thermal behavior of a thermo-pneumatic actuation unit in a micropump. Two alternatives to approach this problem have been studied: first one is a partitioned analysis of the dynamic behavior by looking at different frequency ranges which permits to identify and avoid the problem by ensembling a complete transfer function by a final step of non-linear least-squares fitting in the frequency domain. The second alternative is based in a non-uniform time-stepping in the time domain, but uniform in the logarithm of time. In this way an artifact free transfer function can be obtained over a wide frequency range with minimum computation effort. Finally, this transfer function can be used by an electrical solver with analog behavioral capabilities to obtain the simulation of the complete system.

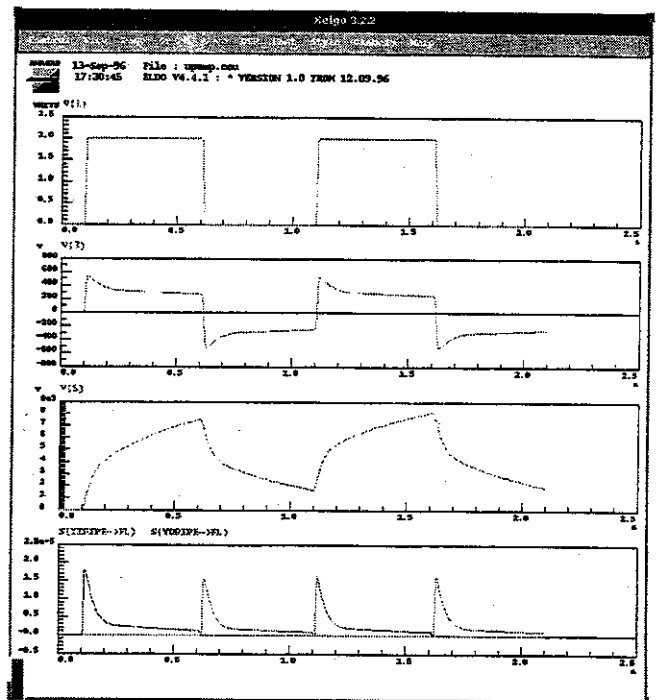


Fig. 11 HDLA micropump results: Power(W), Pressure in the liquid(din/cm²), Air pressure (din/cm²), and liquid flow (cm³/s).

VII. REFERENCES

1. M. Carmona, S. Marco, J. Samitier, J.R. Morante, Dynamic Simulations of Micropumps, *Journal of Micromechanics and Microengineering* 6 pp.128-130, (1996)..
2. L. Ljung, *System Identification* Prentice Hall, Englewood-Cliffs, (1987)
3. ANSYS User Manual version 5.2 1995
4. O.C. Zienkiewicz, R.L. Taylor, *Finite Element Method*, 4th edition McGraw-Hill, (1989).
5. J.O. Smith, *Techniques for Digital Filter Design and System Identification with Application to the Violin*, Ph.D. Dissertation, Stanford University (1983).
6. V. Szekely, T. Van Bien, *Fine Structure of Heat Flow Path in Semiconductor Devices: A measurement and Identification Method*, *Solid-St. Electronics*, 31, (1988).
7. S. Marco, J. Samitier, J.R. Morante, A novel time-domain method to analyse multicomponent exponential transients, *Meas. Sci. Technol.* 6, 135-142, (1995).
8. S. Marco, J. Palacín, A. Guibernau, J. Samitier, Improved multiexponential transient spectroscopy by iterative deconvolution, *Proceedings Instrumentation and Measurement Technology Conference*, (1998).
9. M. Carmona, S. Marco, H. Nguyen, U. Lundquist, A. Pardo, J. Samitier, *Proceedings of the 3rd Advanced Training Course: Mixed-Design of Integrated Circuits and Systems*, Lodz (Poland) A Behavioral Model for the Dynamic Simulation of Micromachined Thermo-Pneumatic Pumps, pp. 458-465, (1996)..